AAS 97–106

LISSAJOUS ORBITS AROUND HALO ORBITS

G. Gómez[†], J. Masdemont[‡] and C. Simó[†]

The analysis of the phase space around the collinear equilibrium points of the Restricted Three Body Problem shows different kinds of motions in a (large) vicinity of these points, depending on the values of the energy. Beyond some critical value of the energy, there appear: an almost vertical periodic orbit that crosses the $z = 0$ plane through a point close to the equilibrium point position, a family of Lissajous orbits around the almost vertical periodic orbits, two halo orbits which are symmetric with respect to the z=0 plane and two families of Lissajous orbits around these halo orbits. Finally, the planar Lyapunov orbit "closes" the level of energy. Halo orbits, which are three dimensional periodic orbits around the equilibrium points are useful, as nominal orbits, for space missions and this is one of the main reasons to study this kind of motions or other ones close to them. This paper is devoted to the study of the two dimensional tori around halo orbits on which the motion is quasiperiodic with two basic frequencies. The orbits look like Lissajous curves. The first part of the paper is devoted to the computation of these orbits using the Lindstedt-Poincaré method. In the second part we study the validity of the formal expansions obtained.

INTRODUCTION

Libration orbits in a vicinity of the collinear equilibrium points have been proved to be suitable for space missions. A global picture, giving all the possibilities of motion near these libration points, can be useful for the analysis of future missions.

Even in a Restricted Three Body Problem (RTBP) model, and using just numerical integration, it is difficult to get an idea of the flow in the vicinity of these points. This is due to two reasons: the first one is the number of degrees of the problem, which makes the explorations rather long, and the second one is the unstable character of the solutions near these equilibrium points.

The instability can be skipped and the degrees of freedom reduced by what is called the reduction to the central manifold. The main ideas of this reduction are as follows: Using suitable coordinates of position, (x_1, x_2, x_3), and momenta, (y_1, y_2, y_3), the Hamiltonian of the RTBP in a vicinity of a collinear equilibrium point is expanded in power series as

$$H = \lambda x_1 y_1 + \frac{1}{2}\omega_1(x_2^2 + y_2^2) + \frac{1}{2}\omega_2(x_3^2 + y_3^2) + H_3 + H_4 + \cdots = H_2 + H_3 + H_4 + \cdots,$$

† Departament de Matemàtica Aplicada i Anàlisi, Universitat de Barcelona, Gran Via 585, 08007 Barcelona, Spain

‡ Departament de Matemàtica Aplicada I, Universitat Politècnica de Catalunya, E.T.S.E.I.B., Diagonal 647, 08028 Barcelona, Spain

where H_k denote homogeneous polynomials of degree k in the above variables. For a fixed value of the RTBP mass parameter, the values of λ, ω_1 and ω_2 depend on the equilibrium point considered. Of the above three terms in H_2, the first one is related to the unstable behaviour of the equilibrium point, and the other ones to librations in the plane of the motion of the primaries and in the out of plane direction.

The first step of the reduction to the central manifold consists in removing, from the full Hamiltonian H, all the terms of the form $x_1^k y_1^l$ with $k \neq l$. This is done performing canonical changes of variables using the Lie series method. The new Hamiltonian (whose variables are denoted again by $(x_1, x_2, x_3, y_1, y_2, y_3)$) has $I = x_1 y_1$ as a first integral, and the reduction to the central manifold is accomplished by setting $x_1 = y_1 = 0$. An alternative procedure removes only the terms with $k + l = 1$, and the central manifold is obtained in the same way (see [7]). What we finally get is a reduced Hamiltonian $\bar{H}(x_2, x_3, y_2, y_3)$ without the unstable term $\lambda x_1 y_1$ and with only two degrees of freedom.

Since the instability is skipped, we can perform long numerical integrations to get an idea of the phase space. Using $x_3 = 0$ with $\dot{x}_3 > 0$ as surface of section, the behaviour of the Poincaré map for a fixed value of the Hamiltonian, can be plotted. In figure 1 we show a typical picture of this map in the vicinity of the L_2 libration point of the Earth-Moon system [5]. See [3] for similar results for the L_1 point of the Earth+Moon–Sun system. The Moon is located outside the figure, in the negative part of the vertical symmetry axis.

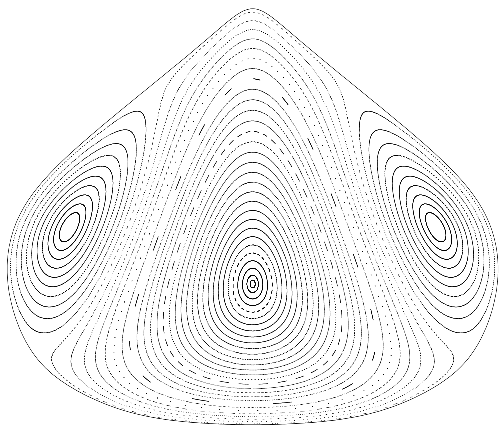

Figure 1: Poincaré map on the central manifold in the vicinity of L_2 libration point of the Earth-Moon system.

The fixed point in the central part of the figure corresponds to an almost vertical periodic orbit (essentially related to the frequency ω_2). The two fixed points at both sides of the plot represent the two symmetric halo orbits having the selected energy. The boundary of the plot is a Lyapunov planar orbit (essentially related to the frequency ω_1, and unstable even in the central manifold). Both around the vertical periodic orbit and around the halo orbits we see invariant curves which represent the intersections of 2D invariant tori, usually filled by quasiperiodic orbits, with the surface of section. These orbits are also known as nonlinear Lissajous orbits. The inner ones are Lissajous orbits around the almost vertical periodic orbit, and the left and right hand side ones are Lissajous orbits around the halo orbits. We shall also refer to them as quasihalo orbits. Between the three families of 2D tori described, there are rather small chaotic zones associated to the stable/unstable manifolds of the planar Lyapunov orbit.

In this paper we present a semianalytical method, based on a Lindstedt-Poincaré (from now on LP) procedure, to compute the 2D tori around a halo orbit. Halo orbits are identified by the *normalized z–amplitude*, that is, the amplitude of the first harmonic in the expansion of the z variable, expressed in normalized coordinates (see later). For small amplitudes they can also be uniquely identified by the frequency. Given a halo orbit of frequency ω, the series obtained for any one of the coordinates, $x(t)$, $y(t)$ and $z(t)$, are of the form

$$\sum_i \left(\sum_{k,m} c_i^{km} \begin{array}{c} \cos \\ \sin \end{array} (k(\omega t + \phi_1) + m(\nu t + \phi_2)) \right) \gamma^i.$$

These expansions depend on two frequencies, ω and ν, and one amplitude, γ. This amplitude is related to the size of the torus around the "base" halo orbit, which is taken as backbone. Later on we shall comment on possible "normalizations" in the definition of γ. The frequency ν is the second natural frequency of the torus, and it is close to the normal frequency around the base halo orbit.

Strictly speaking, these series are asymptotic but divergent everywhere. The high order resonances, which produce the small stochastic zones associated with the divergence, show up only when the expansion is carried up to the order of the resonances. Their effect, for moderate time intervals, is rather small. The computed series have usually been truncated at order 25, and several tests have been done in order to compute a "practical" radius of convergence in terms of γ and depending on the base halo orbit.

Finally we point out that it is also possible to obtain the Lissajous orbits around the halo orbits after a reduction of the Hamiltonian to the central manifold. This is also convenient to obtain the local expansions of the stable and unstable manifolds of these orbits, but we shall not take this approach in the present paper.

HALO ORBITS AS EQUILIBRIUM POINTS

In order to apply the LP method to compute the two dimensional tori around a halo orbit, it is convenient to perform a change of variables which transforms the halo orbit to an equilibrium point of the equations of motion. Then, orbits librating around the equilibrium point in the new coordinates, correspond to orbits librating around the halo orbit in the original ones.

As one can guess, the halo orbit used as backbone becomes an equilibrium point via a time dependent translation. In the new variables the equations of motion are non autonomous, and the complexity of the problem increases. As halo orbits are periodic, the time dependence in the new equations of motion will be also periodic. The expansions of the equations, which must be done in the LP procedure, will have periodic coefficients too. Moreover, the computation of the libration orbits around the equilibrium point of these new equations, can not be done via the LP method unless the linear part has constant coefficients. This requirement is fulfilled via a Floquet change of variables. In this section we are going to show how the previous mentioned translation and Floquet change of variables are done.

The equations of motion of the spatial RTBP where the small primary, of mass μ, is located at $(\mu - 1, 0, 0)$ and the big one, with mass $1 - \mu$, at $(\mu, 0, 0)$ are

$$\ddot{X}_1 - 2\dot{X}_2 = \Omega_{X_1}, \;\; \ddot{X}_2 + 2\dot{X}_1 = \Omega_{X_2}, \;\; \ddot{X}_3 = \Omega_{X_3},$$

$$\Omega(X_1, X_2, X_3) = \frac{1}{2}(X_1^2 + X_2^2) + \frac{1-\mu}{r_1} + \frac{\mu}{r_2},$$

where $X = (X_1, X_2, X_3)$ are the usual *adimensional synodical coordinates* with the origin at the centre of mass and $r_1^2 = (X_1 - \mu)^2 + X_2^2 + X_3^2$, $r_2^2 = (X_1 - \mu + 1)^2 + X_2^2 + X_3^2$.

We denote the collinear equilibrium points by L_1, L_2 and L_3. They are located between the primaries, in the negative part of the X_1 axis and in the positive part of the X_1 axis, respectively.

A preliminary change of coordinates allows to expand the equations of motion in power series around any of the mentioned equilibrium points (see [6], [3]). Denoting by $x = (x_1, x_2, x_3)$ the adimensional coordinates around a selected equilibrium point, L_i, the change of variables to the new ones, denoted as *normalized coordinates*, is given by

$$X_1 = \mp\psi x_1 + \mu + a, \quad X_2 = \mp\psi x_2, \quad X_3 = \psi x_3,$$

where the upper sign corresponds to L_1 and L_2 whilst the lower one to L_3. The value of a is, respectively, $-1+\psi$, $-1-\psi$ and ψ for L_1, L_2 and L_3, and ψ is the distance from the equilibrium point to the nearest primary. It can be computed solving the corresponding Euler's quintic equation. For instance, for L_1 we have

$$\psi^5 - (3-\mu)\psi^4 + (3-2\mu)\psi^3 - \mu\psi^2 + 2\mu\psi - \mu \quad = \quad 0.$$

In these coordinates, and using series expansions around the origin, the equations of motion can be written in the form (see [6])

$$\begin{aligned}
\ddot{x}_1 - 2\dot{x}_2 - (1+2c_2)x_1 &= \frac{\partial}{\partial x_1}\sum_{n\geq 3} c_n\rho^n P_n\left(\frac{x_1}{\rho}\right), \\
\ddot{x}_2 + 2\dot{x}_1 + (c_2-1)x_2 &= \frac{\partial}{\partial x_2}\sum_{n\geq 3} c_n\rho^n P_n\left(\frac{x_1}{\rho}\right), \qquad (1)\\
\ddot{x}_3 + c_2 x_3 &= \frac{\partial}{\partial x_3}\sum_{n\geq 3} c_n\rho^n P_n\left(\frac{x_1}{\rho}\right),
\end{aligned}$$

where $\rho^2 = x_1^2 + x_2^2 + x_3^2$, P_n is the Legendre polynomial of degree n and c_n are constants, depending only on μ, defined by

$$c_n \quad = \quad \frac{1}{\psi^3}\left[\mu + (-1)^n(1-\mu)\left(\frac{\psi}{1+\psi}\right)^{n-1}\right]$$

in the L_1 case, and in a similar way in the other two cases. The equations (1) are the starting point for our computations. Since a great amount of symbolic manipulation must be done, it is convenient to write down the right hand part of these equations using functions which can be computed (and stored) in a fast and easy way. Following [3] this is done using the functions

$$T_n(x_1, x_2, x_3) = \rho^n P_n\left(\frac{x_1}{\rho}\right), \quad \text{and} \quad R_{n-1}(x_1, x_2, x_3) = \frac{1}{x_2}\frac{\partial T_{n+1}}{\partial x_2}.$$

It is not difficult to see that T_n and R_n are polynomials of degree n, satisfying

$$R_{n-1}(x_1, x_2, x_3) = \frac{1}{x_3}\frac{\partial T_{n+1}}{\partial x_3}, \quad \text{and} \quad \frac{\partial T_{n+1}}{\partial x_3} = (n+1)T_n.$$

Using T_n and R_n the equations become

$$\begin{aligned}
\ddot{x}_1 - 2\dot{x}_2 - (1+2c_2)x_1 &= \sum_{n\geq 2} c_{n+1}(n+1)T_n, \\
\ddot{x}_2 + 2\dot{x}_1 + (c_2-1)x_2 &= x_2 \sum_{n\geq 2} c_{n+1} R_{n-1}, \\
\ddot{x}_3 + c_2 x_3 &= x_3 \sum_{n\geq 2} c_{n+1} R_{n-1},
\end{aligned} \tag{2}$$

where R_n and T_n can be obtained using the recurrences that follow from the properties of the Legendre polynomials,

$$\begin{aligned}
T_n(x_1,x_2,x_3) &= \left(2-\frac{1}{n}\right) x_1 T_{n-1} - \left(1-\frac{1}{n}\right)\rho^2 T_{n-2}, \\
R_n(x_1,x_2,x_3) &= \frac{2n+3}{n+2} x_2 R_{n-1} - \frac{2n+2}{n+2} T_n - \frac{n+1}{n+2}\rho^2 R_{n-2},
\end{aligned}$$

starting with $T_0 = 1$, $T_1 = x_1$, $R_0 = -1$ and $R_1 = -3x_1$.

Denoting by $x = (x_1, x_2, x_3, x_4, x_5, x_6) \equiv (x_1, x_2, x_3, \dot{x}_1, \dot{x}_2, \dot{x}_3)$, the equations of motion (2) can be written in compact form as $\dot{x} = f(x)$.

Assume that $\bar{x}(t) = (\bar{x}_1(t), \bar{x}_2(t), \bar{x}_3(t), \dot{\bar{x}}_1(t), \dot{\bar{x}}_2(t), \dot{\bar{x}}_3(t))$ is a halo orbit, solution of the equations (2). The time dependent change of variables $x = z + \bar{x}$ transforms $\dot{x} = f(x)$ into $\dot{z} + \dot{\bar{x}} = f(z + \bar{x})$. Expanding $f(z+\bar{x})$ in power series around the halo orbit we get

$$f(z+\bar{x}) = f(\bar{x}) + A(\bar{x})z + g(z,\bar{x}),$$

where $A(\bar{x})$ is a time dependent matrix and $g(z,\bar{x})$ is a function whose Taylor series expansion in powers of z_i, $i = 1 \ldots 6$, starts at order two and has time dependent coefficients. Both A and g can be obtained by symbolic manipulation.

Since the halo orbit is a solution of the initial equations we have $\dot{\bar{x}} = f(\bar{x})$, and so

$$\dot{z} = A(\bar{x}(t))z + g(z, \bar{x}(t)), \tag{3}$$

where the linear part of this equations, $\dot{z} = A(\bar{x}(t))z$, gives rise to the variational equations around the halo orbit.

The fact that the halo orbit is periodic implies that the time dependence in (3) is also periodic. In this way, the halo orbit $\bar{x}(t)$, can be seen as a function of an angle Φ_1, $\bar{x}(\Phi_1)$, where $\Phi_1 = \omega t + \phi_1$, being ω the frequency of the halo orbit and ϕ_1 a phase. If T denotes the period of the halo orbit then $T\omega = 2\pi$.

In order to apply the LP procedure, it is advisable that the matrix A of (3) be constant. As its time dependence is periodic, it can be removed via a Floquet change of coordinates. This is a linear change with periodic coefficients, that we note by $z = Py$, where $P = P(\Phi_1)$ is a periodic matrix.

Introducing $z = Py$ in (3) we get $\dot{P}y + P\dot{y} = APy + g(Py, \Phi_1)$, that is

$$\dot{y} = (P^{-1}AP - P^{-1}\dot{P})y + P^{-1}g(Py, \Phi_1).$$

The matrix P is computed by solving $\dot{P} = AP - PB$, where B is known as the Floquet matrix. B is a constant matrix which is a logarithm of the monodromy matrix of $\dot{z} = A(\bar{x}(t))z$ divided by the period T (see [1]). In this way equations (3) become

$$\dot{y} = By + Qg(Py, \Phi_1), \tag{4}$$

where $Q = P^{-1}$. The matrix B, after a suitable change of basis, can be simplified to

$$B = \begin{pmatrix} 0 & 0 & 0 & 1 & 0 & 0 \\ 0 & 0 & 0 & 0 & 1 & 0 \\ 0 & 0 & 0 & 0 & 0 & 1 \\ b_{41} & 0 & b_{43} & 0 & b_{45} & 0 \\ 0 & 0 & 0 & b_{54} & 0 & b_{56} \\ b_{61} & 0 & b_{63} & 0 & b_{65} & 0 \end{pmatrix}. \tag{5}$$

Note that the final equations (4) can be obtained from the original ones (2) using the linear change of variables

$$x = P(\Phi_1)y + \bar{x}(\Phi_1). \tag{6}$$

THE LINDSTEDT-POINCARÉ PROCEDURE

In this section we are going to explain how we can compute the quasihalo orbits of the equations (4) by means of a LP method.

First of all, we note that the equations $\dot{x} = f(x)$ of the RTBP at the equilibrium point have $f_1 = f_2 = f_3 = 0$ and so in (4) $g_1 = g_2 = g_3 = 0$. The system (4) can be written as

$$\begin{pmatrix} \dot{y}_1 \\ \dot{y}_2 \\ \dot{y}_3 \\ \dot{y}_4 \\ \dot{y}_5 \\ \dot{y}_6 \end{pmatrix} = \left(\begin{array}{ccc|ccc} & & & 1 & & \\ & 0 & & & 1 & \\ & & & & & 1 \\ \hline b_{41} & 0 & b_{43} & 0 & b_{45} & 0 \\ 0 & 0 & 0 & b_{54} & 0 & b_{56} \\ b_{61} & 0 & b_{63} & 0 & b_{65} & 0 \end{array}\right) \begin{pmatrix} y_1 \\ y_2 \\ y_3 \\ y_4 \\ y_5 \\ y_6 \end{pmatrix} + Q \begin{pmatrix} 0 \\ 0 \\ 0 \\ g_4(Py) \\ g_5(Py) \\ g_6(Py) \end{pmatrix}, \tag{7}$$

Where the g functions depend periodically on time (directly and through P).

Using the first three equations we obtain,

$$\dot{y}_j \;\; = \;\; y_{j+3} + \sum q_{j,i+3} g_{i+3}(Py), \;\; j = 1, 2, 3, \tag{8}$$

and in all the sums, from now on and unless otherwise stated, i runs from 1 to 3.

Taking derivatives with respect to time we have, for $j = 1, 2, 3$,

$$\dot{y}_{j+3} \;\; = \;\; \ddot{y}_j - \sum \dot{q}_{j,i+3} g_{i+3}(Py) - \sum q_{j,i+3} \dot{g}_{i+3}(Py).$$

Inserting these derivatives into the last three equations of (7) and making use of (8), we get

$$\begin{aligned} \ddot{y}_1 - b_{41}y_1 - b_{43}y_3 - b_{45}\dot{y}_2 \;\; &= \;\; -b_{45} \sum q_{2,i+3} g_{i+3}(Py) + \\ & \sum \left(\dot{q}_{1,i+3} g_{i+3}(Py) + q_{1,i+3} \dot{g}_{i+3}(Py) + q_{4,i+3} g_{i+3}(Py) \right), \\ \ddot{y}_2 - b_{54}\dot{y}_1 - b_{56}\dot{y}_3 \;\; &= \;\; -\sum \left(b_{54} q_{1,i+3} + b_{56} q_{3,i+3} \right) g_{i+3}(Py) + \\ & \sum \left(\dot{q}_{2,i+3} g_{i+3}(Py) + q_{2,i+3} \dot{g}_{i+3}(Py) + q_{5,i+3} g_{i+3}(Py) \right), \\ \ddot{y}_3 - b_{61}y_1 - b_{63}y_3 - b_{65}\dot{y}_2 \;\; &= \;\; -b_{65} \sum q_{2,i+3} g_{i+3}(Py) + \\ & \sum \left(\dot{q}_{3,i+3} g_{i+3}(Py) + q_{3,i+3} \dot{g}_{i+3}(Py) + q_{6,i+3} g_{i+3}(Py) \right), \end{aligned} \tag{9}$$

where the left hand side contains the linear part and the right hand one the higher order terms. Note that in these equations Py, which appears in the functions g_j, still contains the variables y_4, y_5, y_6, implying that (9) are coupled with (8).

As the goal of a LP procedure is to get a formal series solution of equations (4), we can proceed doing the following steps, to be explained later in more detail.

- Start by computing the solution of the linear part of (9). As we will see, this gives the order one of the series expansion of y_1, y_2, y_3.
- Use (8) to determine y_4, y_5, y_6 up to order one. Up to this order we have $y_4 = \dot{y}_1$, $y_5 = \dot{y}_2$, $y_6 = \dot{y}_3$.
- Assume that y_1, y_2, y_3, y_4, y_5, y_6 have been determined up to a certain order $n-1$.
- Use (9) and the usual algorithm of the LP procedure to determine the order n of y_1, y_2, y_3. Note that, since the right hand side part of (9) begins with quadratic terms in Py, for this step we need only y_1, y_2, y_3, y_4, y_5, y_6 up to order $n-1$, to equate the terms of order n of both sides.
- Using again (8), determine the terms of order n of y_4, y_5, y_6. For this purpose we need y_1, y_2, y_3 up to order n, previously computed, and y_4, y_5, y_6 up to order $n-1$, computed in the preceding iteration.
- Repeat the last three steps up to a desired order N (to be defined later).

Taking into account the type of series (sinus o cosinus) for the halo orbit $\bar{x}$, for the entries of P and the relation (6) one gets that y_1, y_3 and y_5 will be cosinus type series whilst y_2, y_4 and y_6 will be sinus type ones. The series expansions for y_j, $j = 1, ..., 6$, are searched in the following way,

$$y_j(t) \quad = \quad \sum_{i=1}^{\infty} \left(\sum_{k,m} y_{j,i}^{k,m} \begin{array}{c} \cos \\ \sin \end{array} (k\Phi_1 + m\Phi_2) \right) \gamma^i. \tag{10}$$

For the angles Φ_1 and Φ_2 we use the expressions,

$$\Phi_1 = \omega t + \phi_1, \qquad \Phi_2 = \nu t + \phi_2,$$

where Φ_1 is the same as in the halo orbit, this is, ω is the frequency of the backbone halo orbit. The frequency ν is related to the motion of the Lissajous orbit around the halo one. Due to the nonlinear character of equations (7) it can not be kept fixed but depending on the amplitude γ, which essentially measures the displacement from the quasihalo orbit to the base halo one selected, so, it is expanded in the form

$$\nu = \sum_{i=0}^{\infty} \nu_i \gamma^i. \tag{11}$$

Giving arbitrary values to the phases ϕ_1, ϕ_2 and to the amplitude γ (this one inside the range of "convergence" which will be studied later) we obtain all the Lissajous orbits around a halo orbit which have one of the fundamental frequencies equal to the one of the halo. One notices at this point that $\gamma = 0$ implies $y = 0$ and by (6), the solution that we get is the halo orbit. Moreover, due to the autonomous character of the RTBP, one can fix one of the phases equal to zero and, by varying γ and the other phase, the same set of solutions is obtained.

Assuming the halo orbit expanded as an infinite Fourier series, the range for k in (10) goes from 0 to ∞. During the procedure only y terms with $|m| \leq i$ and $k \equiv i \pmod 2$ show up. Also only terms ν_i with i even appear. Since the expansions of the halo orbit are truncated to l harmonics, only terms with $k \leq l$ are kept in the expansions. Moreover when $k = 0$, changing the sign of the coefficient if necessary, only terms with $m \geq 0$ are kept. All these facts have been taken into account in the semianalytical implementation in order to save computing time and storage.

Also the sum with respect i in (10) must be truncated at some value N, $(N \leq l)$, which will be known as the *order* of the final expansion. At the n-th step of the procedure the terms with $i = n$ of the y variables are determined. We say that at this step we have the solution up to order n meaning that if we insert formally into (4), the expansions obtained for the residuals, which are of the same type as (10), are zero for all the terms with $k \leq l$ and $i \leq n$. The solutions to order N have been, first, formally tested by inserting them into (4) and checking that it holds up to order N.

Computation of the linear part

The linear part of (9) is

$$\begin{aligned} \ddot{y}_1 - b_{41}y_1 - b_{43}y_3 - b_{45}\dot{y}_2 &= 0, \\ \ddot{y}_2 - b_{54}\dot{y}_1 - b_{56}\dot{y}_3 &= 0, \\ \ddot{y}_3 - b_{61}y_1 - b_{63}y_3 - b_{65}\dot{y}_2 &= 0. \end{aligned} \tag{12}$$

A non trivial librating solution of these equations must be used to determine the coefficients of (10) with $i = 1$. This is, we are looking for the expansions up to order one of y_j, $j = 1, 2, 3$, denoted by y_j^1, with

$$y_j^1(t) = \gamma \sum_{k,m} y_{j,1}^{k,m} \begin{matrix}\cos \\ \sin\end{matrix} (k\Phi_1 + m\Phi_2).$$

Since (12) does not depend on the halo frequency ω we must take $y_{j,1}^{k,m} = 0$, $j = 1, 2, 3$, for $k \neq 0$. Taking into account the restrictions on the index, only $y_{j,1}^{0,1}$, $j = 1, 2, 3$, remain as free coefficients. So, for all γ and ϕ_2, we must look for a non trivial solution of the form

$$y_j^1(t) = \gamma y_{j,1}^{0,1} \begin{matrix}\cos \\ \sin\end{matrix} (\nu t + \phi_2).$$

When these expressions are required to satisfy (12) one finds

$$\begin{pmatrix} -(b_{41}+\nu^2) & -b_{45}\nu & -b_{43} \\ b_{54}\nu & -\nu^2 & b_{56}\nu \\ -b_{61} & -b_{65}\nu & -(b_{63}+\nu^2) \end{pmatrix} \begin{pmatrix} y_{1,1}^{0,1} \\ y_{2,1}^{0,1} \\ y_{3,1}^{0,1} \end{pmatrix} = \begin{pmatrix} 0 \\ 0 \\ 0 \end{pmatrix}.$$

Since a non trivial solution is needed, the value of $\nu \neq 0$ making the determinant of the former linear system equal to zero, must be selected. This is easily found solving,

$$\nu^4 + (b_{65}b_{56} + b_{54}b_{45} + b_{41}b_{63})\nu^2 + b_{41}b_{63} - b_{43}b_{61} + b_{65}b_{56}b_{41} + b_{54}b_{45}b_{63} - b_{54}b_{65}b_{43} - b_{61}b_{45}b_{56} = 0.$$

The root of this equation gives the term ν_0 in the expansion of ν given by (11). As the linear system is homogeneous, one has one free parameter in the determination of the coefficients

$y_{j,1}^{0,1}$, $j = 1, 2, 3$. This freedom is related to the different possible "normalizations" in the definition of the parameter γ. We have selected γ as the coefficient of $\cos(\nu t + \phi_2)$ in the Fourier expansion of y_3. This gives $y_{3,1}^{0,1} = 1$ having, in this way, an unique solution for the linear part. Concerning the higher order terms, this choice implies $y_{3,n}^{0,1} = 0$ for all $n > 1$. Any other choice can be reduced to this one by a suitable redefinition of γ, a fact which is assured by using the implicit function theorem.

Now we have the expansions of y_1, y_2 and y_3 up to order one,

$$y_1^1(t) = \gamma y_{1,1}^{0,1} \cos(\nu_0 t + \phi_2), \quad y_2^1(t) = \gamma y_{2,1}^{0,1} \sin(\nu_0 t + \phi_2), \quad y_3^1(t) = \gamma y_{3,1}^{0,1} \cos(\nu_0 t + \phi_2).$$

Finally, using (8) we get the terms of y_4, y_5 and y_6 of order one. In this case we have $y_{4,1}^{k,m} = y_{5,1}^{k,m} = y_{6,1}^{k,m} = 0$ for $k \neq 0$ and $y_{4,1}^{0,1} = -\nu_0 y_{1,1}^{0,1}$, $y_{5,1}^{0,1} = \nu_0 y_{2,1}^{0,1}$ and $y_{6,1}^{0,1} = -\nu_0 y_{3,1}^{0,1}$.

Computation of the higher order terms

To compute the higher order terms we proceed recursively. Assume that at a certain step we have y_j, $j = 1, ..., 6$, determined up to order $n-1$ and ν up to order $n-2$ (resp. $n-3$) if $n-1$ is odd (resp. even) (in fact we can assume ν determined up to order $n-2$ since otherwise, when it is only determined up to order $n-3$, then $n-2$ is odd and $\nu_{n-2} = 0$).

The insertion of these known terms in the right hand side of (9) produces expansions which are completely known up to order n. Denote them by $\bar{r}_{1,n}^{k,m}$, $\bar{r}_{2,n}^{k,m}$ and $\bar{r}_{3,n}^{k,m}$. Note that they are series as the ones in (10), of cosinus, sinus and cosinus type respectively. They can be computed, given the expansions of x_1, x_2 and x_3 up to order $n-1$, via the change of variables (6), and making use of the recurrences for T_j and R_j which appear in the equations (2). Note that the series for x_1, x_2 and x_3 are the final goal of our computations and they are of the same type as y_1, y_2 and y_3, respectively.

The purpose of the first part of the n-th step is to equate terms of order n at both sides of (9). Up to now we have computed the order n of the right hand side. Now we must compute the order n of the left hand side. This is made of an unknown part of order n and a known one that must be determined and added to $\bar{r}$.

Denote by s any one of the y functions. The derivatives with respect to time, which appear in the left hand side of equations (9), can be computed by

$$\begin{aligned} \dot{s} &= \frac{\partial s}{\partial \Phi_1}\frac{d\Phi_1}{dt} + \frac{\partial s}{\partial \Phi_2}\frac{d\Phi_2}{dt} = \omega\frac{\partial s}{\partial \Phi_1} + \nu\frac{\partial s}{\partial \Phi_2}, \\ \ddot{s} &= \omega^2\frac{\partial^2 s}{\partial \Phi_1^2} + \omega\nu\frac{\partial^2 s}{\partial \Phi_1 \partial \Phi_2} + \nu^2\frac{\partial^2 s}{\partial \Phi_2^2}, \end{aligned}$$

where we recall that ω is constant but ν is given by the series (11).

Since any partial derivative of s is formally a series like the ones in (10), the products of ν by partial derivatives are series products. Moreover, ν^2 is also a series product which is of the same type as (11). The order n of a series product that appear in our computations is computed multiplying the part of order j of a frequency type series (11) by the part of order $n-j$ of an expansion type series like (10) and then, adding the results from $j = 0$ to $j = n-1$ (we note that the series like (10) have no zero order part).

When j ranges from $j = 1$ to $n-2$ in the products of ν by a partial derivative, there appear known terms. In a similar way there appear known terms in the computation of ν^2 which are used later when computing $\nu^2 \frac{\partial^2 s}{\partial \Phi_2^2}$ for the same values of j. Assume that all these values are added to the corresponding $\bar{r}_1^n$, $\bar{r}_2^n$ and $\bar{r}_3^n$.

When $j=0$ or $j=n-1$ the following table summarizes the terms that appear for $\dot{s}$ and $\ddot{s}$. The symbol δ stands for Kronecker's delta.

j	$n-j$	$\dot{s}$	$\ddot{s}$
0	n	$\pm(k\omega+m\nu_0)s_n^{k,m}$	$-(k\omega+m\nu_0)^2 s_n^{k,m}$
$n-1$	1	$\pm\nu_{n-1}s_1^{0,1}\delta_{k,0}\delta_{m,1}$	$-2\nu_0\nu_{n-1}s_1^{0,1}\delta_{k,0}\delta_{m,1}-N_{n-1}^2 s_1^{0,1}\delta_{k,0}\delta_{m,1}$

In the table, the $\pm$ sign has to be taken $+$ (resp. $-$) if s is a sinus (resp. cosinus) series. N_{n-1}^2 represents the known part of ν^2 of order $n-1$, obtained multiplying the parts of order j of ν with the ones of order $n-2$ from $j=1$ to $n-2$. $s_j^{k,m}$ stands for the term (k,m) of the part of order j of the series s.

Note that the term $N_{n-1}^2 s_1^{0,1}\delta_{k,0}\delta_{m,1}$ in the previous table is known. So, all the contributions coming from these terms in the second derivatives of the y series in the left hand side of (9) can be included in the series $\bar{r}$. From now on we denote by r_1^n, r_2^n and r_3^n the part of order n of the respectives initial series, $\bar{r}$, updated with the known part of order n coming from the left hand side of equations (9). Following the usual notation, we refer to the individual terms by $r_{1,n}^{k,m}$, $r_{2,n}^{k,m}$ and $r_{3,n}^{k,m}$.

By equating the terms of order n in both sides of (9) we obtain the linear system

$$\begin{aligned}
-\left(\Psi^2+b_{41}\right)y_{1,n}^{k,m}-b_{45}\Psi y_{2,n}^{k,m}-b_{43}y_{3,n}^{k,m}-(2\nu_0 y_{1,1}^{0,1}+b_{45}y_{2,1}^{0,1})\nu_{n-1}\delta_{k,0}\delta_{m,1} &= r_{1,n}^{k,m}, \\
b_{54}\Psi y_{1,n}^{k,m}-\Psi^2 y_{2,n}^{k,m}+b_{56}\Psi y_{3,n}^{k,m}+(b_{54}y_{1,1}^{0,1}+b_{56}y_{3,1}^{0,1}-2\nu_0 y_{2,1}^{0,1})\nu_{n-1}\delta_{k,0}\delta_{m,1} &= r_{2,n}^{k,m}, \\
-b_{61}y_{1,n}^{k,m}-b_{65}\Psi y_{2,n}^{k,m}-\left(\Psi^2+b_{63}\right)y_{3,n}^{k,m}-(2\nu_0 y_{3,1}^{0,1}+b_{65}y_{2,1}^{0,1})\nu_{n-1}\delta_{k,0}\delta_{m,1} &= r_{3,n}^{k,m},
\end{aligned}$$

where $\Psi=k\omega+m\nu_0$. It must be solved for the unknowns $y_{1,n}^{k,m}$, $y_{2,n}^{k,m}$, $y_{3,n}^{k,m}$ and ν_{n-1}.

When $(k,m)\neq(0,1)$ it becomes

$$\begin{pmatrix} -b_{41}-\Psi^2 & -b_{45}\Psi & -b_{43} \\ b_{54}\Psi & -\Psi^2 & b_{56}\Psi \\ -b_{61} & -b_{65}\Psi & -b_{63}-\Psi^2 \end{pmatrix}\begin{pmatrix} y_{1,n}^{k,m} \\ y_{2,n}^{k,m} \\ y_{3,n}^{k,m}\end{pmatrix}=\begin{pmatrix} r_{1,n}^{k,m} \\ r_{2,n}^{k,m} \\ r_{3,n}^{k,m}\end{pmatrix}, \tag{13}$$

from which we get $y_{1,n}^{k,m}$, $y_{2,n}^{k,m}$ and $y_{3,n}^{k,m}$.

We note that the case $(k,m)=(0,0)$ gives a singular matrix, but it is easily solved taking $y_{2,n}^{0,0}=0$, since r_2 is a sinus type series and so $r_{2,n}^{0,0}=0$.

When $(k,m)=(0,1)$ (that only happens when n is odd) the matrix of (13) is singular, since in the computations of the first order part we selected ν_0 in that way. But in this case the additional contribution of ν_{n-1} gives

$$\begin{pmatrix} -b_{41}-\nu_0^2 & -b_{45}\nu_0 & -b_{43} & -2\nu_0 y_{1,1}^{0,1}-b_{45}y_{2,1}^{0,1} \\ -b_{54}\nu_0 & -\nu_0^2 & b_{56}\nu_0 & b_{54}y_{1,1}^{0,1}+b_{56}y_{3,1}^{0,1}-2\nu_0 y_{2,1}^{0,1} \\ -b_{61} & -b_{65}\nu_0 & -b_{63}-\nu_0^2 & -2\nu_0 y_{3,1}^{0,1}-b_{65}y_{2,1}^{0,1}\end{pmatrix}\begin{pmatrix} y_{1,n}^{0,1} \\ y_{2,n}^{0,1} \\ y_{3,n}^{0,1} \\ \nu_{n-1}\end{pmatrix}=\begin{pmatrix} r_{1,n}^{0,1} \\ r_{2,n}^{0,1} \\ r_{3,n}^{0,1}\end{pmatrix}.$$

There is an unique value of ν_{n-1} such that this system is solvable. Then it remains one free parameter to determine $y_{1,n}^{0,1}$, $y_{2,n}^{0,1}$ and $y_{3,n}^{0,1}$. We set $y_{3,n}^{0,1}=0$, as mentioned in the discussion of the solution of the linear part, avoiding all ambiguities.

Finally we must compute the series of order n of y_4, y_5 and y_6. For this purpose we use (8). Note that for the computations we need y_1, y_2 and y_3 up to order n and y_4, y_5 and y_6 up to order $n-1$.

A SAMPLE OF THE ORBITS OBTAINED

Using the procedure developed in the last section, we have done computations of quasi-halo orbits for different situations: Earth+Moon–Sun and Earth–Moon systems and L_1, L_2 equilibrium points. We shall present here the results corresponding to the Earth+Moon–Sun system, L_1 point. All the computations were done up to order 25, both in γ and in the order of the Fourier harmonics.

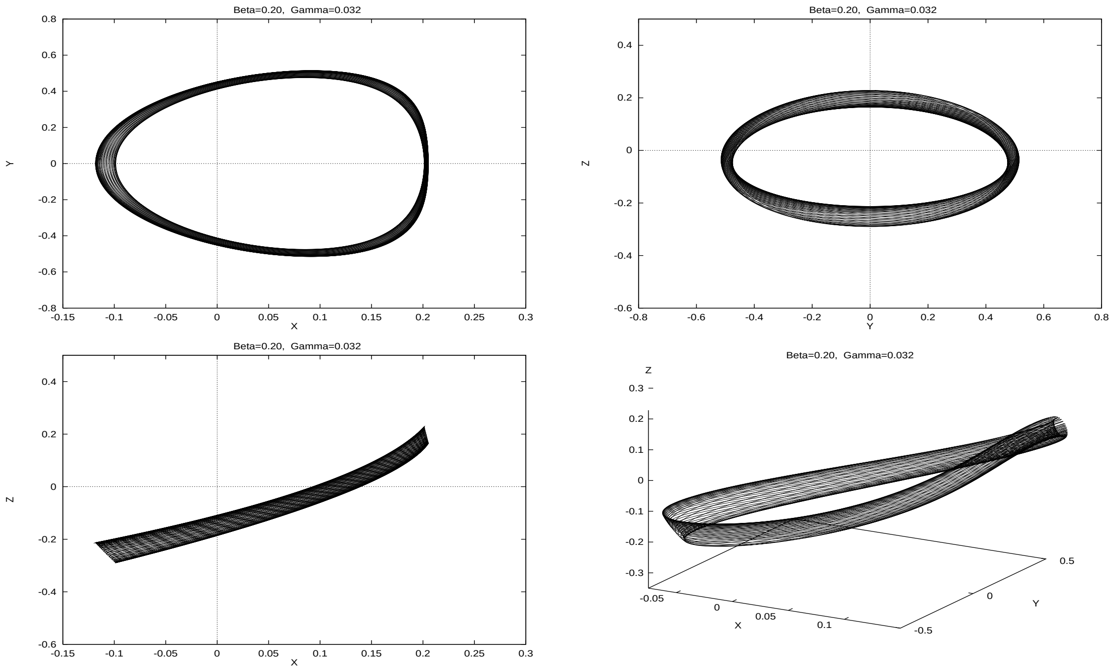

Figure 2: Projections on the coordinate planes and a 3D representation of the quasihalo orbit with $\beta = 0.2$ and $\gamma = 0.032$.

As a sample of the results obtained, figures 2, 3, 4 and 5 show the projections on the coordinate planes of some orbits. All of them have been computed taking as backbone halo orbit one with amplitude $\beta = 0.2$ and the four plots show quasihalo orbits with different γ amplitudes. The first one, in figure 2, has $\gamma = 0.032$ and the motion is clearly quasiperiodic on a small torus around the halo orbit. Figure 3 corresponds to $\gamma = 0.067$. For this value of the amplitude, there is a resonance between ω and ν, and the motion on the torus is periodic. Some of these periodic motions, but for the Lissajous orbits around the vertical periodic orbit, can be seen in figure 1. Figure 4 is similar to figure 2, but with a larger value of γ, in this case very close to the border of the "practical region of convergence", as we shall see later. Finally, figure 5 shows an orbit having some strange bendings, also computed with the procedure. For this orbit, the value of γ is outside the practical region of convergence. All the orbits have been plotted for a time span corresponding to 40 revolutions of the base halo orbit. This means 122 adimensional time units or, equivalently, 19.5 years.

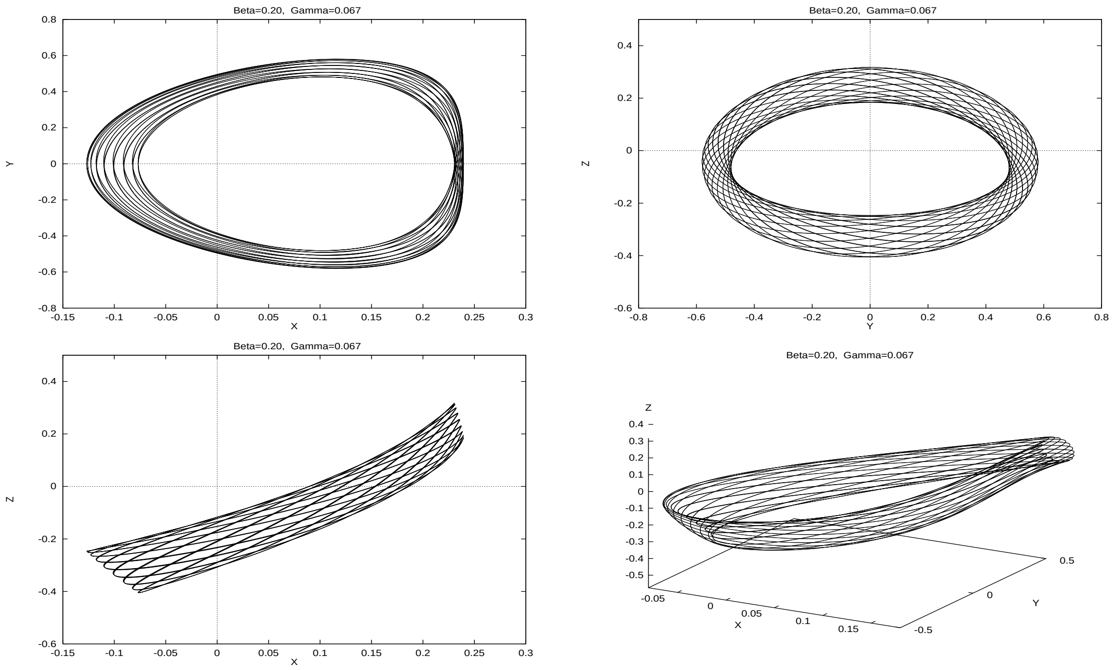

Figure 3: Projections on the coordinate planes and a 3D representation of the quasihalo orbit with $\beta = 0.2$ and $\gamma = 0.067$. For this value of γ we have resonance between the two frequencies and so the motion is periodic.

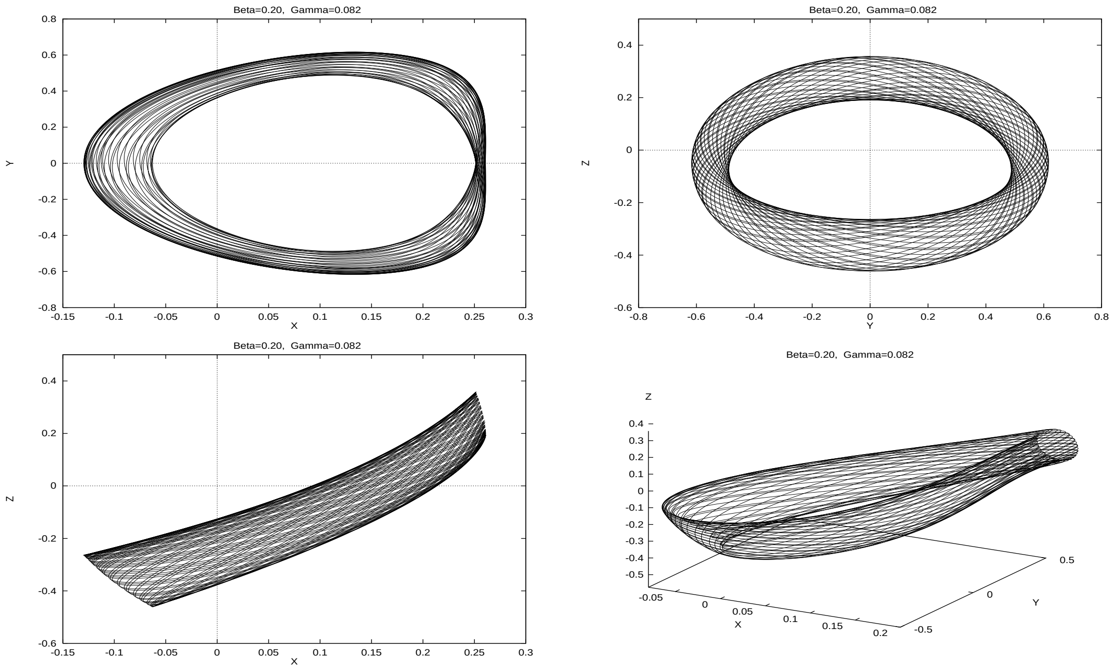

Figure 4: Projections on the coordinate planes and a 3D representation of the quasihalo orbit with $\beta = 0.2$ and $\gamma = 0.082$. This value of γ is close to the border of the region of convergence of the expansions.

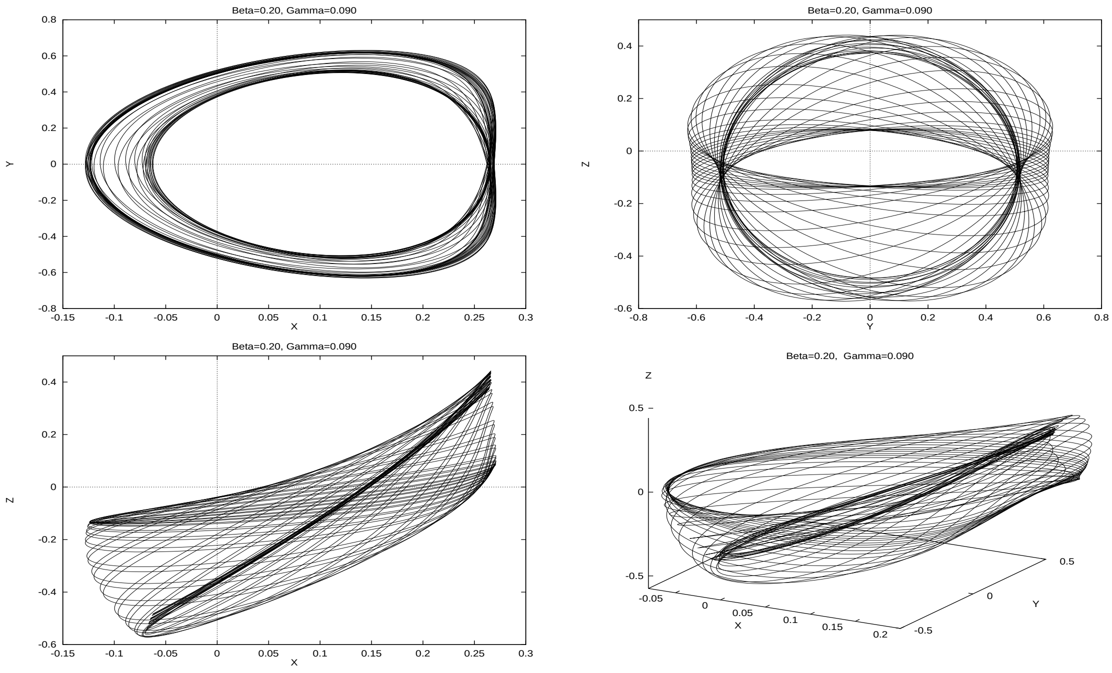

Figure 5: Similar to the previous figures for $\beta = 0.2$ and $\gamma = 0.090$. For this value of γ the expansions are out of the range of convergence.

To have an idea of the thickness, we have plotted the intersections of these tori with the surface of section $z = 0$, $\dot{z} > 0$, for different amplitudes. The results are shown in figure 6. In the left hand side figure, the points on the different "curves" correspond to the quasihalo orbits with γ =0.02, 0.03, 0.04 and 0.05. All the motions are clearly quasiperiodic and the orbits associated to each one of the curves fill up the corresponding torus. The points on the orbits of the right hand side figure, are (close to) periodic. For the amplitudes selected there is a resonance between the halo frequency and the normal one to the halo which is close to 17:1 for the outer points (γ =0.067), 20:1 for the intermediate points (γ =0.051) and 23:1 for the inner points (γ =0.035). These two plots have a pattern very different from the one displayed in figure 1. This is due to several reasons. The first is that in figure 6 the coordinates used are the x, y synodical coordinates, while in figure 1 are not (a short explanation of the changes of coordinates done to produce the figure is given at the Introduction). The second point is that in figure 1 the value of the Hamiltonian is fixed for all the orbits of the plot (see [5]), and this is not the case in figure 6. If we want to produce a picture similar to figure 1, we must also keep the value of the energy fixed. This is what we have done in figure 7. In this figure, the value of the energy, given by the Hamiltonian of the RTBP in normalized units and assigning the value zero to the L_1 point, is $h = 0.6$, which is the one corresponding to the periodic halo orbit with $\beta = 0.2$ (300 000 km approximately). This orbit should be represented as a fixed point of the Poincaré map siting inside all the curves. The other curves correspond to quasihalo orbits of different values of γ, but that have been computed for different values of β, in order to be on a fixed level of the energy.

In figure 8 we have represented the values of the two basic frequencies associated to the tori: the halo frequency, ω, and the frequency, ν. In the left figure we plot both frequencies (the halo one decreased by 2.05 units, only for representation purposes) for different values of β. In this plot, for the frequency ν we have only taken the constant term, ν_0, of the series (11). That is, ν_0 is the normal frequency associated to the halo orbit. In the figure on the right, for different values of the normalized z-amplitude, β, between 0.05 and 0.25, the variations with γ of the ν frequency are shown. The variations are rather small in all cases, associated to different base halo orbits.

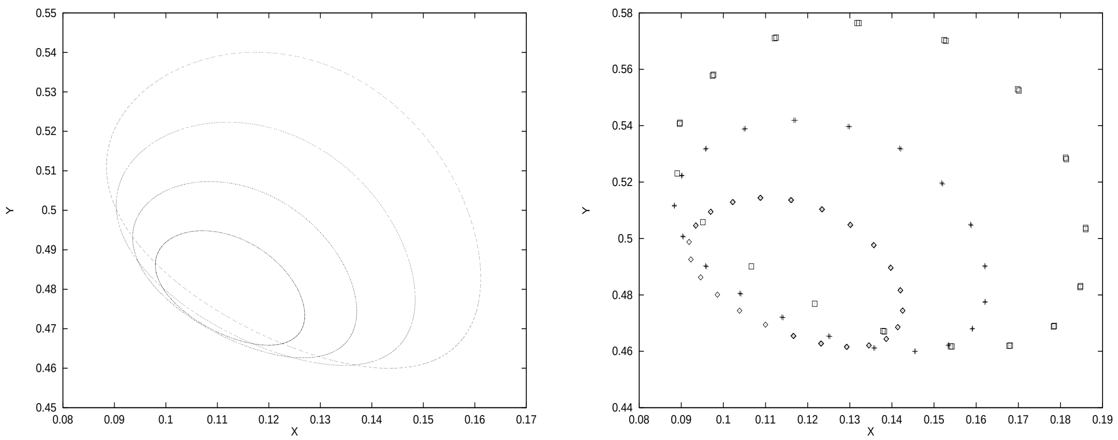

Figure 6: Intersections of the quasihalo orbits with $z = 0$, $\dot{z} > 0$. All the orbits have β=0.2. In the left figure the different "curves" correspond to γ =0.02 (inner curve), 0.03, 0.04, 0.05 (outer curve). In the right figure the values of γ (0.035 in the inner curve, 0.051 and 0.067 in the outer curve) are such that the motion on the tori is very close to periodic.

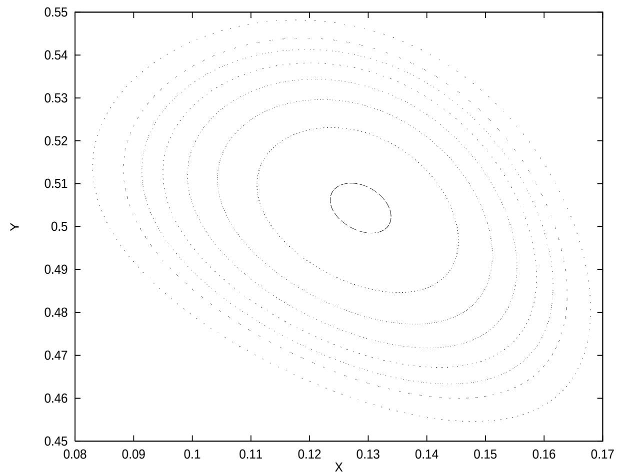

Figure 7: Intersection of the quasihalo orbits with $z = 0$. All the orbits have the same value of the Hamiltonian, $h = 0.6$. Inside all the curves there is a fixed point of the Poincarè map, corresponding to a halo orbit with $\beta = 0.2$. The different curves correspond to quasihalo orbits with γ =0.18 (inner curve), 0.20, 0.21, 0.22,...,0.26 (outer curve).

CONVERGENCE OF THE SERIES

From figure 1 it is clear that the quasiperiodic Lissajous orbits under consideration do not exist for arbitrary values of the amplitude γ. In fact, the size of the region, around the

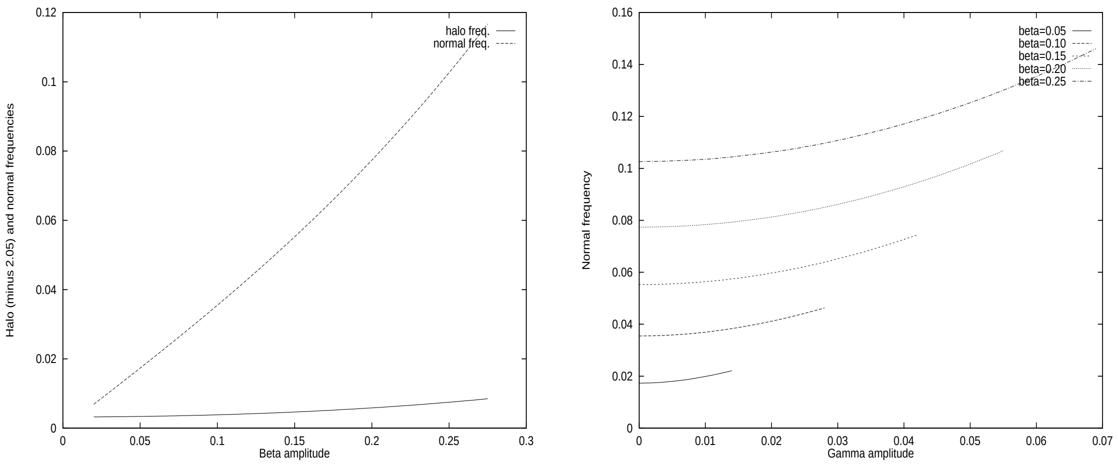

Figure 8: In the left figure we plot, for different β amplitudes, the frequency of the halo orbit (minus 2.05) and the normal frequency ν_0. On the right figure, for different values of β (0.05, 0.10, 1.15, 0.20 and 0.25), the corresponding ν frequency of the quasihalo orbit, when the γ amplitude varies, is represented.

fixed point associated with the halo orbit, varies with the energy or, equivalently, with the amplitude of the backbone halo orbit. On the other hand, the series that we have produced for these orbits (up to order 25) are asymptotic but divergent everywhere. This is due to the fact that do not exists any open set foliated by 2D tori. Nevertheless, the resonances, which produce small stochastic zones associated with the divergence, show up only when the expansion is carried up to the order of the resonances. So their "practical" effect, for moderate time intervals, is rather small and can be neglected. On the other hand, standard KAM arguments can be used to prove rigorously the existence of these Lissajous orbits (see [4].)

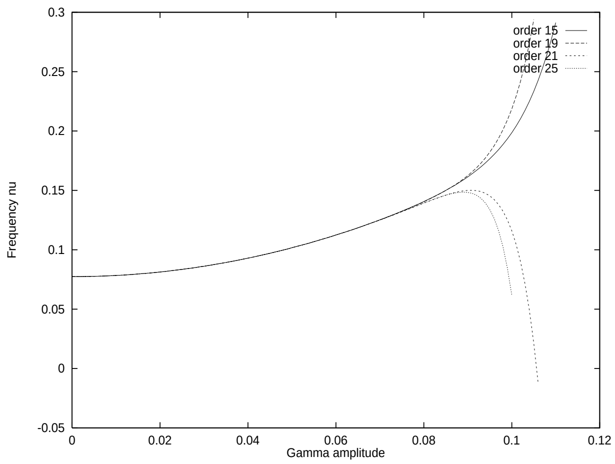

Figure 9: For $\beta = 0.20$, ν frequencies computed using different order for the expansions. The differences become significant for values of γ greater than 0.08, approximately, which corresponds to the practical radius of convergence.

We have computed a "practical" radius of convergence in terms of the amplitude γ, for different values of the amplitude β of the reference halo orbit. For these tests we have used the series of the ν frequency computed up to order 25. For a fixed value of β, as a first estimate, we can compute γ truncating the series (11) at different orders. This is shown in figure 9 for β=0.20. The values obtained with the different truncations are in good agreement up to values of γ approximately equal to 0.08. This value can be taken as a first approximation for the convergence radius.

If we apply the quotient criterion to the series (11), it is seen that the values of the quotients of consecutive coefficients tend in a fast way to a stabilizing value. We have used the maximum and minimum values of these quotients, when their values are close to the last one, as upper and lower estimates of the radii of convergence. These are the values that are represented in figure 10 for different values of β. For β=0.2, the value of the radius is 0.084 which is close to the estimate obtained before. When, for a fixed value of β, γ varies between zero and the most pessimistic estimate for the radii of convergence, we can compute the energy of the different orbits given by the value of the Hamiltonian. In this way, we can represent a domain of "practical convergence" in the (β-h) plane, where h is the value of the Hamiltonian. The dotted points of the right hand side picture of figure 10 determine this region. In this figure, if we cut the dotted region with the horizontal line h=0.6, we can determine the range of values for the amplitude β of the orbits that were plotted in figure 7.

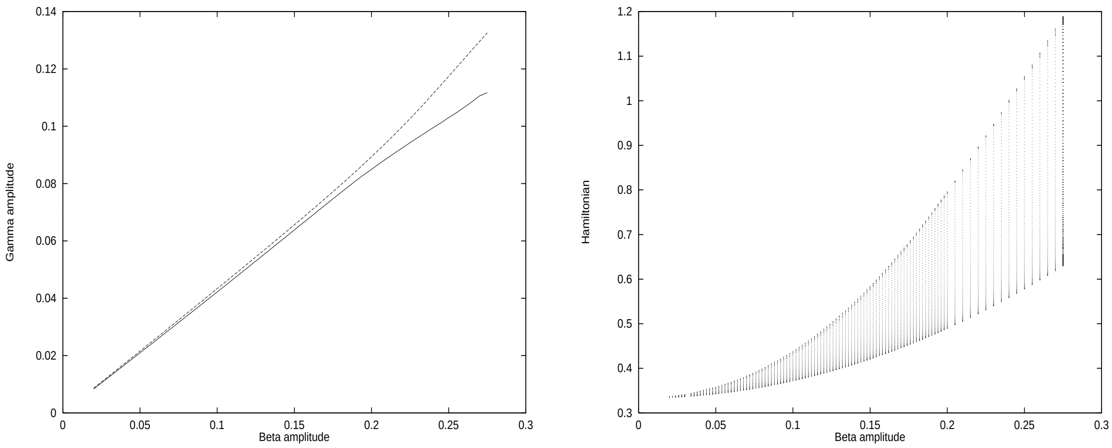

Figure 10: Upper and lower estimates for the practical radius of convergence of ν, for different values of β. In the left figure it is given in terms of the γ amplitude and in the right figure in terms of the value of the Hamiltonian. In the right figure the lower boundary of the dotted region corresponds to the halo orbits ($\gamma = 0$).

As a test for the goodness of the computed solutions, we have done the following numerical experiments. We can compare the solutions obtained with the LP procedure with those computed by numerical integration of the differential equations of the RTBP taking, of course, the same initial conditions. We fix a certain maximum separation in the configuration space, and we stop the integration when this separation is reached. We have done the comparison using the expansions for the quasihalo orbits up to order 25.

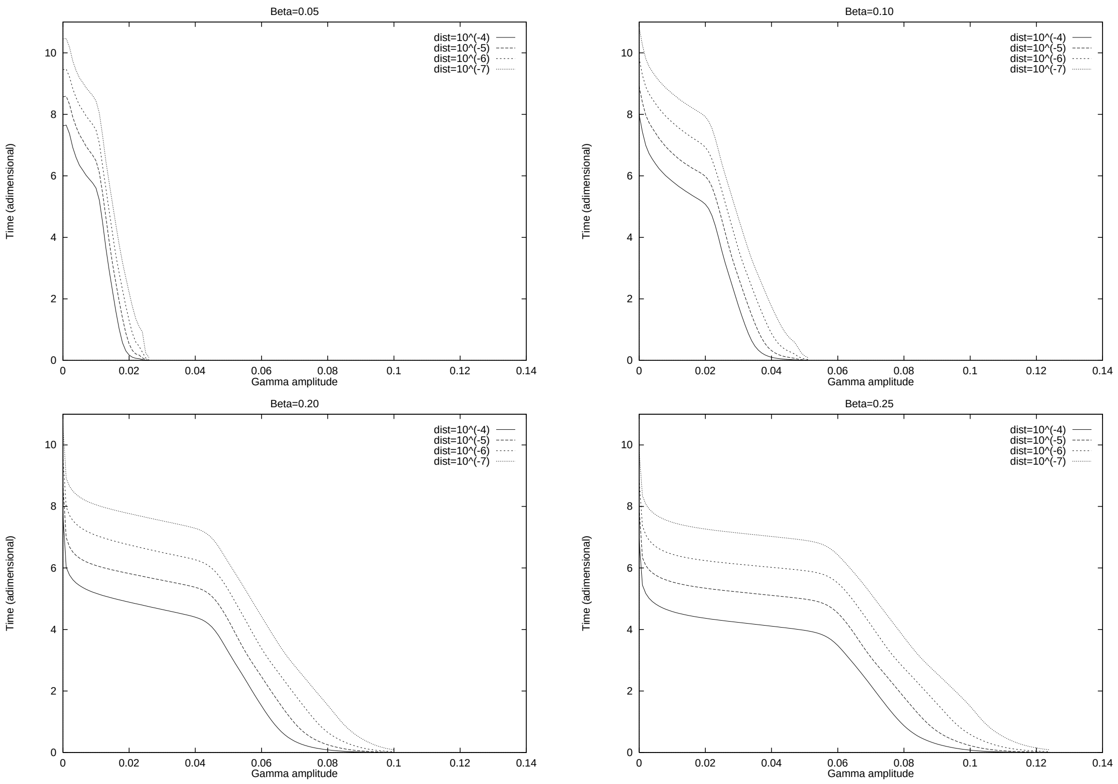

Figure 11: γ vs escape time for different distances. The different curves displayed in each one of the figures show the escape time versus γ when varying the distance adopted as escape distance. The values taken are 15, 150, 1 500 and 15 000 km. All the computations have been done using order 25 for the expansions. The different figures correspond to different values of β: 0.05, 0.10, 0.20 and 0.25.

In figure 11 the results are shown taking as maximum separation the values 15 000, 1 500, 150 and 15 km. The computations have been done for different values of the amplitude of the base halo orbit, and varying, for each one, γ. Of course, in all cases one should have escape, because of the strong intrinsic instability of these orbits. For a fixed value of β, and moving in the sense of decreasing values of γ, if we are in the non convergence region the escape is very fast. When the boundary of the "convergence" zone is reached, the orbits remain nearby for a time interval that varies between 4 and 9 adimensional time units (2π adimensional units = 1 year). This variation depends mainly on the maximum separation allowed, and very mildly on the size of the base halo orbit, given by its z-amplitude β. After this, the escape is very fast due to the highly unstable character of the solutions considered. The explorations have been done for a large set of initial conditions, obtained by varying the initial phases at the initial epoch. The results are close to those presented here, that correspond to both phases equal to zero.

Concerning the instability properties of the quasihalo orbits, they are essentially the same as the ones of the base halo orbits: When β increases, the orbits become less unstable, but in all cases they display a strong instability. However the spacecraft can be easily controlled in practice by rather cheap station-keeping strategies. The related geometric ideas and the technical details can be found, in the case of halo orbits, in [2] and [3].

CONCLUSIONS

A method to compute Lissajous orbits around the halo orbits near the collinear libration points in the RTBP has been introduced. It is based on a variant of the classical Lindstedt-Poincaré method. The full procedure is given in detail. To demonstrate the feasibility, the required symbolic manipulation software has been developed, implemented and ran on several examples. Exhaustive tests concerning the domain of applicability and direct numerical verifications have been done. An alternative procedure, based on a previous reduction to the central manifold is pointed out. From this one can conclude that a new methodology is available to enlarge the set of candidates to nominal orbits, ready to be used for future space missions in an extended vicinity of the collinear libration points associated to any couple of primaries.

ACKNOWLEDGEMENTS

This work has been supported by DGICYT Grant PB 94–0215 (Spain). Partial support of the EC grant ERBCHRXCT940460, and the catalan grant CIRIT 1996S0GR-00105 is also acknowledged.

References

[1] Coddington E.A., Levinson N., *Theory of Ordinary Differential Equations*, Mc Graw-Hill, New York 1955.

[2] Gómez, G., Llibre, J., Martínez, R., Simó, C., *Station keeping of libration point orbits*, Final Report. ESOC Contract NO: 5648/83/D/JS(SC), 1985.

[3] Gómez, G., Jorba, À., Masdemont, J., Simó, C., *Study Refinement of Semianalytical Halo Orbit Theory*, Final Report. ESOC Contract NO: 8625/89/D/MD(SC), 1991.

[4] Jorba, À., Villanueva, J., *On the Normal Behaviour of Partially Elliptic Lower Dimensional Tori of Hamiltonian Systems*, Univ. Politècnica de Catalunya, preprint, 1997.

[5] Jorba, À., Masdemont, J., *Nonlinear Dynamics in an Extended Neighbourhood of the Translunar Equilibrium Point*, in *NATO–ASI Hamiltonian Systems with Three or More Degrees of Freedom*, eds. C. Simó, A. Delshams.

[6] Richardson, David L., (1980) Analytic Construction of Periodic Orbits about the Collinear Points. *Celestial Mechanics*, **22**, pp. 241–253.

[7] Simó, C., *Effective Computations in Hamiltonian Dynamics,* in *Cent ans après les Méthodes Nouvelles de H. Poincaré*, Société Mathématique de France, 1–23, 1996.